Model independent measurement of production of two jets with two charged lepton pairs in Large Hadron Collidor at $\sqrt{s} = 13$ TeV

Qichen Dong

December 23, 2019

Abstract

This report

1 Introduction

Vector boson scattering (VBS) process is important as a pure electroweak interaction to probe the nature of electroweak symmetry breaking (EWSB). At the TeV scale, VBS process alone violated the longitudinally unitarity, however, in the standard model (SM), the apparence of higgs boson cancels the violation rigorously. Since higher order effects beyond the SM (BSM) are suppressed tromendusly at low energy scale, study of VBS process in higher energy scale may gives hints of BSM theories which offer alternative EWSB machenisms to break the elegent cancellation of longitudinally unitarity. Moreover, study of the VBS process provides a good chance to observe the CP violating effects that contribute to the large matter antimatter asymetry observed in the universe. Since no CP vioaltion effect is predicted in the SM in the VBS process, only sources of CP violation come from BSM theories which interfere with the SM.

In the Large hardron collidor (LHC), VBS events are produced by a pair of vector bosons which produced by initial partrons scattered into another pair of vector bosons. At detector level, events with two jets associated with 2 pairs of leptons originated from vector bosons pair are the signiture of VBS process. Despite the complexity of final states, background processes other than the VBS can also produce exactly the same final state particles, we denote these processes $jjVV$, one of the main $jjVV$ background is $jjVV$ production with strongly interacting verteices ($S\ jjVV$). The most VBS concentrated channel is $jjVV$ processes with only electroweak verteices, denote as ($EW\ jjVV$). Figure 1 shows example Feynman diagrams of leading order $S\ jjZZ$ and $EW\ jjZZ$ processes[1].

Despite same final state particle in leading order $EW\ jjVV$ and $S\ jjVV$ process, the geometry configuration of them are quite different, Electroweak jjVV production process is expected to have a much larger jets separation since two heavy vector bosons emitted from each of the initial state quarks, while the Strong jjVV production is expected to be more likely to radiate additional jets since quark and gluon carrys color charge. Moreover, the vector bosons produced by EW jjZZ process are more centralised between the two associated jets and more balanced in p_T. These informations were used to define the signal region and control regions in the measurement.

The $EW\ jjVV$ process in which both vector bosons decay leptonically is extremely rare with cross section around $1fb$ in current energy scale, but it is a relatively clean

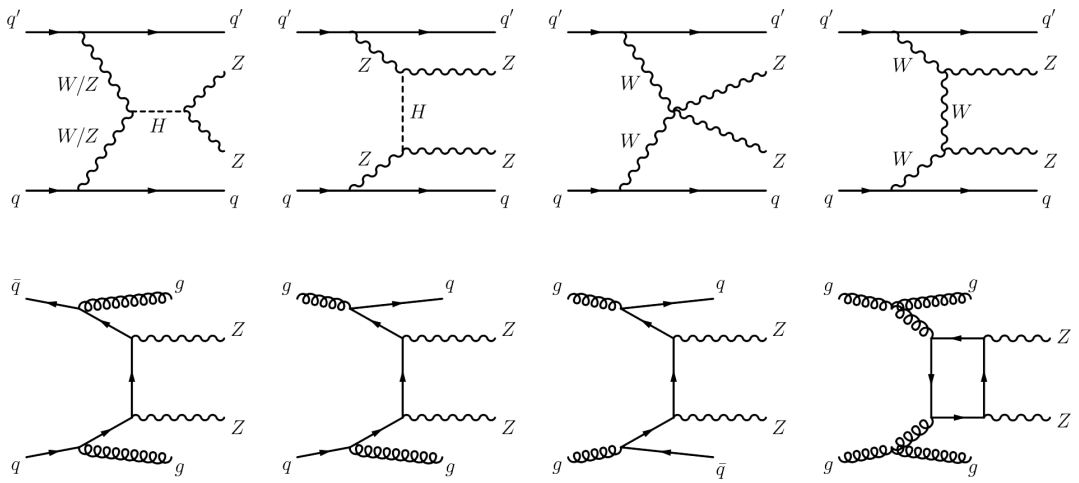

Figure 1: The first order feynman diagrams contributing to $jjZZ$ processes, the first line is $EW\ jjZZ$ and the second line is $S\ jjZZ$ processes.

channel with minimal hardronic background. In this report, only events with final states contain 2 pairs of charged leptons from Z bosons was considered as signal, denote as $jjZZ4l$, other procedures were considered as backgrounds.

In this report, the $36fb^{-1}$ pp collision data with centre of mass energy $\sqrt{s} = 13TeV$ collected by the atlas detector in 2016 is used, the differential cross section of VBS process and irreduceable background in a VBS enhanced fidutial phase space is measured. The experimental effect induced by the detector is removed by unfolding with the help of simulation events, so that the results can be directly compared by future experiments.

2 ATLAS detector

The performance and geometry detail of ATLAS detector can be found in reference[6]. ATLAS detector is a general-purpose layered-design particle detector built in 2008, which is cylindrically symmetric to the beam axis with near complete coverage in solid angle. The first layer, inner tracking detector covering pseudorapidity range $|\eta| < 2.5$ is submerged in 2T axial magnetic field produced by superconducting electromagnet, which is designed to track charged particles. The second layer is the complex of electromagnetic calorimeter and hardroninc calorimeter, where particles interact with

the material and deposit energy, both covering $|\eta| < 3.2$. In the region where $4.9 > |\eta| > 3.2$, a forward electromagnetic and hadronic calorimeters is used. The third layer is the large muon spectrometer covering $|\eta| < 2.7$, due to the high penetrating power of muon, both calorimeter cannot stop muons, much larger apperatus is used to capture their track. Around 25 pp collides (2016) in the center of the detector each time beams cross the detector, resulting around 1 billion collisions per second, most of which are elastic collision contain little information, complicate hardware and software online trigger system[11] is used to cutdown events rate to about 1000 per second for analyists to study offline. A cut-away view of the ATLAS detector with main components labeled is shown in Figure 1[6].

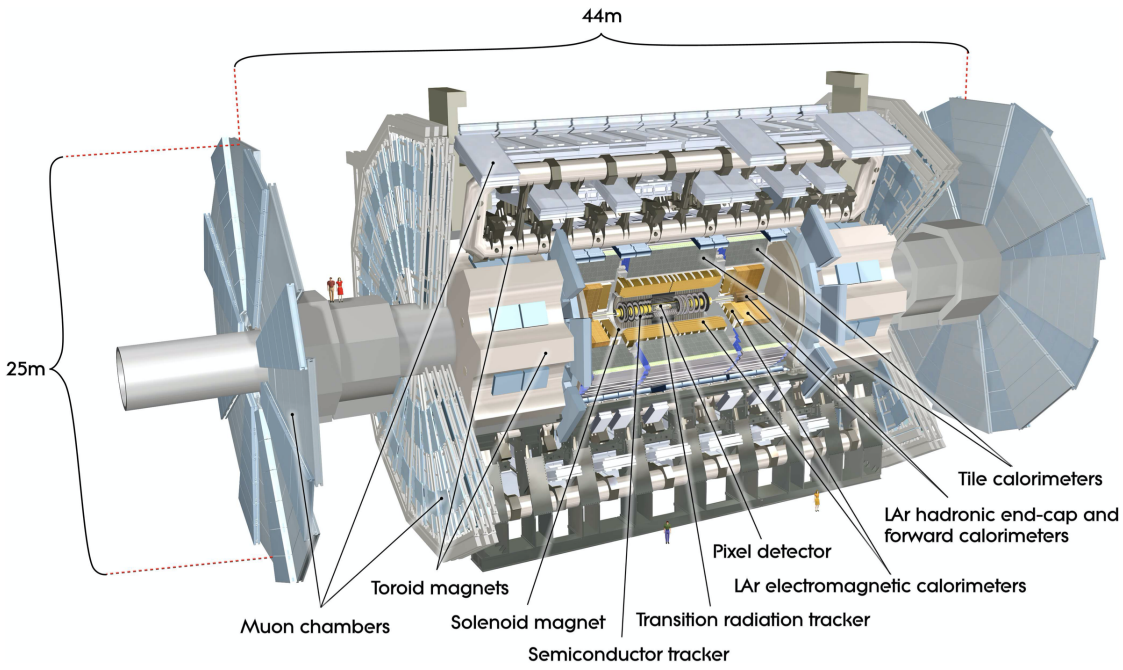

Figure 2: A cut-away wiew of the ATLAS detector, major components and the dimension of it is labeled.

3 Data and Simulation

The measurement is performed using the pp collision data recorded during 2015 and 2016 run of LHC with $\sqrt{s} = 13\ TeV$. During this peroid, an integrated luminosity

of $36fb^{-1}$ is obtained. Data taken in 2017 and 2018 run can be used in the future for further analysis.

Simulation for various processes used in the measurement are generated by different Monte Carlo (MC) generators, three generations of simulation events corresponding to 3 years of LHC run with different pile up and integrated luminosity are available, adding up to simulation data corresponding to a total of $139fb^{-1}$. Only the simulation data corresponding to 2015-2016 run was used in this measurement to have best prediction to the data. The $EWjjZZ$ process is modeled by Sherpa2.2.2[7] with NNPDF3.0NNLO[4] partron distribution function (PDF) at leading order (LO). The vector boson fusion (VBF) higgs contribution is modeled using POWHEGVBF_H[8] configuration with Pythia8[10] showering and NNPDF3.0 PDF.

The $S\ qq \to jjZZ$ process is generated by Sherpa2.2.2 with NNPDF30NNLO PDF, events with less then 2 jets are generated at next to LO(NLO), others are generated at LO, while $t\bar{t} \to H \to ZZ$ contribution is generated separately by POWHEG[9] with Pythia8 showering and NNPDF2.3 PDF. The $S\ gg \to jjZZ$ process is modeled using Sherpa2.2.2 with NNPDF30NNLO PDF, again, the $gg \to H \to ZZ$ is modeled separately with POWHEG and Pythia8.

The production of $jjWZ$ events is produced by POWHEG with Pythia8. The EW triboson process with the same order of $\alpha = 6$ is modeled by Sherpa2.2.2 with NNPDF30NNLO PDF. Single Z boson decay is modeled by Sherpa with NNPDF30NNLO PDF while $t\bar{t}Z$ decay is modeled separately with the same configuration. $t\bar{t}$ production is modeled by POWHEG with Pythia8 showering.

All simulations were include detailed detector simulation by Geant4[3]. both simulated events and the data were reconstructed using raw spatial and momentum of leptons and jets in CERN ROOT[5] framework.

4 Candidates selection

selecting the desired $ZZ4l$ events while substracting other background effects is challenging, while distinguishing $EWjjZZ$ and $SjjZZ$ is even harder, the final states of both process are identical but we can still study the differences in geometry information and possible associated process of these events. The selection used in this report is largly similar to the selection detailed in ref. [1].

The detector level selection relies on the properties of all final state particles, namely charged leptons and jets.

Jets within $|\eta| < 2.4$ were required to have transverse momentum (p_T) higher than 30 GeV, jets with higher pseudorapidity $2.4 < |\eta| < 4.5$ must have $p_T > 40$ GeV.

Muons were identified by compatible tracks in the muon spectrometer and the inner tracking detector. outside the region of inner tracking detector, muons can also be identified by an MS track alone. The identified muons described above are required to have $p_T > 7$GeV. Muons are required to have $|\eta| < 2.7$ and satisfy "loose" particle identification criterion. Electrons were identified using the information of the EM calorimeter and corresponding tracks in the inner tracking detector. Electrons is also required to satisfy "loose" identification working point, and have $p_T > 7$GeV and $|\eta| < 2.47$.

A "FixedCutPflowLoose" lepton isolation creteria[2] is required by all identified charged leptons to remove leptons overlap with jets. Furthermore, the tracks of leptons were required to have transverse impact parameter d_0 and longitudinal impact parameter z_0 satisfying $d_0/\sigma_{d_0} < 5$ and $z_0 \sin\theta < 0.5$ mm.

TODO::OVERLAP REMOVAL

the resonance of Z boson pair were recostructed by two pairs of same flavor, opposite charge (denote SFOC) leptons passed detector level selection, the tracks of two SFOC lepton pairs are required have separation $\Delta R > 0.2$, where $\Delta R = \sqrt{\Delta\eta^2 + \Delta\phi^2}$, moreover, the three leading leptons with higher p_T are required to have $p_T > 20, 20, 10$ respectively. if more then two candidate OSFC lepton pairs were avilable, the lepton pairs with invarient mass($m_{l^+l^-}$) closest to Z boson mass were selected. the lepton pair with mass closest to Z boson mass are required to have invarient mass $70GeV < m_{Z_1} < 110GeV$ and the other have $21\ GeV < m_{Z_1} < 110GeV$.

Events must have at least two jets pass detector level selection, the leading and subleading jets with $y_{j_1} \times y_{j_2} < 0$ and $|y_{j_1} - y_{j_2}| > 2$ and dijet invarient mass $m_{jj} > 200GeV$ and $P_{Tj_1} > P_{Tj_2} > 30GeV$ were selected.

The $EWjjZZ$ events are predicted to be more balanced in P_T, which is parametrised by

$$P_{T\ balance} = |\frac{P_{T\ jjZZ}}{P_{T\ Z_1} + P_{T\ Z_2} + P_{T\ j_1} + P_{T\ j_2}}|$$

where $P_{T\ jjZZ}$ is the total P_T of the 4 leptons 2 jets system and the denominator is the scalar sum of individual P_T.

With the fiducial phase space defined, signal region (SR) and control regions (CR) are further defined base on centrarity and the apperence of additional jets inbetween (denote $nIBj$) the leading and subleading jets. The centrarity is defined as

$$C_{ZZ} = \frac{y_{jj} - y_{ZZ}}{y_{j_1} - y_{j_2}}$$

which indicates how the Z boson pair system is centraised in the dijet system. In SR region, events are required to have $C < 0.5$ and $nIBj = 0$, outside of which were defined as conjagate CR. Table 1 summarise the SR and CR definition used in the analysis.

5 Cutflow comparasion

In this measurement, three analysits worked on the similar fiducial volumes, while developing different algorithm for events selection. It is valuable to check the consistancy of different implementations. A specific fiducial area and certain order of selecting physical objects were agreed and cutflow diagrams indicating predicted EW jjZZ event number based on simulation after each selection are obtained. Only in this section, the all 3 generations of simulation data were used and the phase space volume is slightly different from which is used in the measurement. Figure *WHICH* shows a cutflow diagram which have been compared with other analyists and turn out to be consistant.

6 Background and uncertainty

The $jjZZ4l$ channel contain 3 major processes, namely $EWZZ4l$, $SqqZZ4l$ and $SggZZ4l$, background process come mainly form process involve top quark, other contributions are small. In this stage of measurement, all processes were modeled using the simulation events, the VH, triboson, WZ process and processes with top quark in leading order can produce same or similar final state with signal process, if leptons or jets was misidentified, they can potentially fake $jjZZ4l$ process, from

Objects	SR	$CR_{C_{ZZ}}$	CR_{jIB}	CR_{all}
Electrons	"Loose" ID criterion "FixedCutPflowLoose" criterion $p_T > 7$ GeV, $\|\eta\| < 2.47$ $\|d_0/\sigma_{d_0}\| < 5$, $\|z_0 \sin\theta\| < 0.5$mm			
Muons	"Loose" ID criterion "FixedCutPflowLoose" criterion $p_T > 7$ GeV, $\|\eta\| < 2.7$ $\|d_0/\sigma_{d_0}\| < 3$, $\|z_0 \sin\theta\| < 0.5$mm			
Jets	$P_T > 30(40)$GeV for $\|\eta\| < 2.4(2.4 < \|\eta\| < 4.5)$			
OSFC lepton pairs	two pairs of OSFC lepton with M_Z closest to Z mass $p_T > 20, 20, 10$ GeV for leading 3 leptons $\Delta R_{l^+l^-} > 0.2$ 70 GeV $< M_{Z_1} <$ 110 GeV 21 GeV $< M_{Z_2} <$ 110 GeV			
Dijets system	leading two jets with $y_{j_1} \times y_{j_2} < 0$ and $\|y_{j_1} - y_{j_2}\| > 2$ dijet invarient mass $M_{jj} > 200$ GeV			
jjZZ system	$C < 0.5$ $nIBj = 0$	$C < 0.5$ $nIBj > 0$	$C > 0.5$ $nIBj = 0$	$C > 0.5$ $nIBj > 0$

Table 1: Summary of selection applied for selecting events in SR and CR phase space.

now on denote "Other" process. there are potential to usr data driven methods to constrain the background in future analysis.

With only detector level selection, the predicted distribution of 4-lepton imvarient mass (M_{4l}) is shown in Figure 4, in which we can clearly see the single Z boson resonance around 91 GeV dominated by $Sqq4l$ process, Higgs resonance around 125 GeV dominated by $SggH4l$ process, and the "shoulder" of Z boson pair mass starting from about 182 GeV.

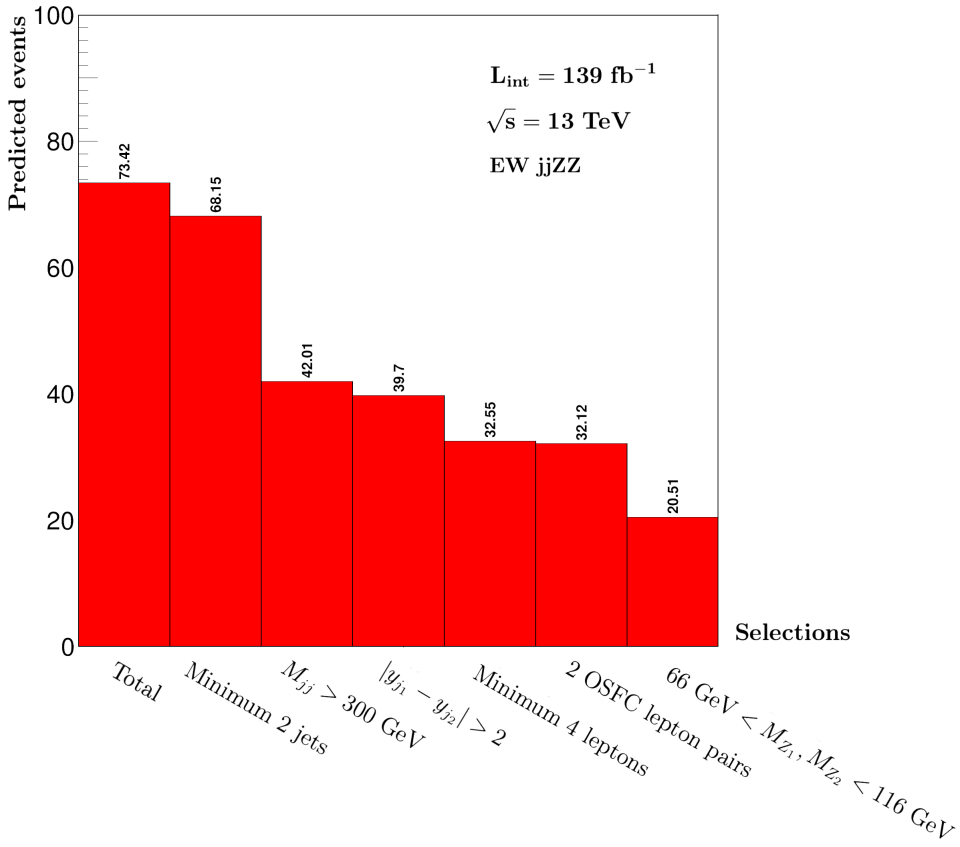

Figure 3: Cutflow diagram of the predicted $EW\ jjZZ$ event number after selection cuts. Uncertainty was omitted and numbers after the decimal point were preserved.

7 detector effect removal

why unfold and how, limitations; and its results.

8 Discussion

what further work can be done. (preunfold, setlimits, more data, CP violation)

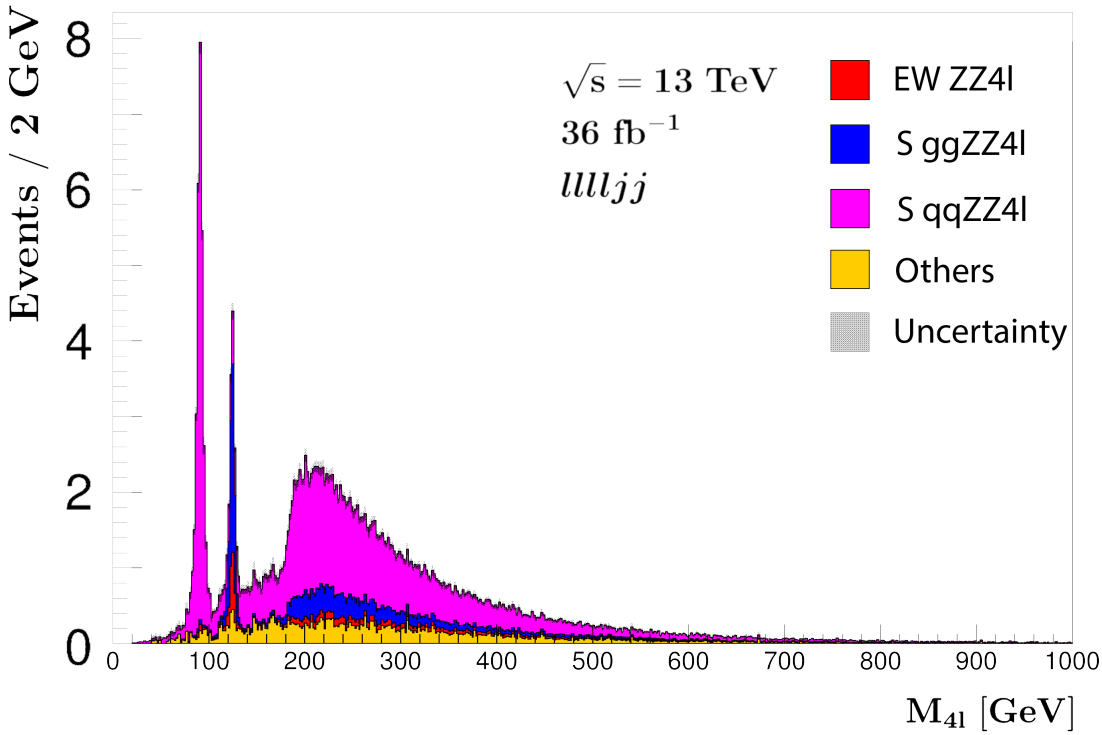

Figure 4: Predicted M_{4l} distribution, with main resonance features shown clearly.

9 Conclusion

References

[1] Observation of electroweak production of two jets in association with a Z-boson pair in pp collisions at $\sqrt{s} = 13$ TeV with the ATLAS detector. Technical Report ATLAS-CONF-2019-033, CERN, Geneva, Jul 2019.

[2] M. Aaboud, G. Aad, B. Abbott, D. C. Abbott, O. Abdinov, B. Abeloos, D. K. Abhayasinghe, S. H. Abidi, O. S. AbouZeid, and et al. Electron reconstruction and identification in the atlas experiment using the 2015 and 2016 lhc proton-proton collision data at $\sqrt{s} = 13$tev. *The European Physical Journal C*, 79(8), Aug 2019.

[3] S. Agostinelli, J. Allison, K. Amako, J. Apostolakis, H. Araujo, P. Arce, M. Asai, D. Axen, S. Banerjee, G. Barrand, F. Behner, L. Bellagamba, J. Boudreau,

L. Broglia, A. Brunengo, H. Burkhardt, S. Chauvie, J. Chuma, R. Chytracek, G. Cooperman, G. Cosmo, P. Degtyarenko, A. Dell'Acqua, G. Depaola, D. Dietrich, R. Enami, A. Feliciello, C. Ferguson, H. Fesefeldt, G. Folger, F. Foppiano, A. Forti, S. Garelli, S. Giani, R. Giannitrapani, D. Gibin, J.J. Gmez Cadenas, I. Gonzlez, G. Gracia Abril, G. Greeniaus, W. Greiner, V. Grichine, A. Grossheim, S. Guatelli, P. Gumplinger, R. Hamatsu, K. Hashimoto, H. Hasui, A. Heikkinen, A. Howard, V. Ivanchenko, A. Johnson, F.W. Jones, J. Kallenbach, N. Kanaya, M. Kawabata, Y. Kawabata, M. Kawaguti, S. Kelner, P. Kent, A. Kimura, T. Kodama, R. Kokoulin, M. Kossov, H. Kurashige, E. Lamanna, T. Lampn, V. Lara, V. Lefebure, F. Lei, M. Liendl, W. Lockman, F. Longo, S. Magni, M. Maire, E. Medernach, K. Minamimoto, P. Mora de Freitas, Y. Morita, K. Murakami, M. Nagamatu, R. Nartallo, P. Nieminen, T. Nishimura, K. Ohtsubo, M. Okamura, S. O'Neale, Y. Oohata, K. Paech, J. Perl, A. Pfeiffer, M.G. Pia, F. Ranjard, A. Rybin, S. Sadilov, E. Di Salvo, G. Santin, T. Sasaki, N. Savvas, Y. Sawada, S. Scherer, S. Sei, V. Sirotenko, D. Smith, N. Starkov, H. Stoecker, J. Sulkimo, M. Takahata, S. Tanaka, E. Tcherniaev, E. Safai Tehrani, M. Tropeano, P. Truscott, H. Uno, L. Urban, P. Urban, M. Verderi, A. Walkden, W. Wander, H. Weber, J.P. Wellisch, T. Wenaus, D.C. Williams, D. Wright, T. Yamada, H. Yoshida, and D. Zschiesche. Geant4a simulation toolkit. *Nuclear Instruments and Methods in Physics Research Section A: Accelerators, Spectrometers, Detectors and Associated Equipment*, 506(3):250 – 303, 2003.

[4] J. Alwall, R. Frederix, S. Frixione, V. Hirschi, F. Maltoni, O. Mattelaer, H. S. Shao, T. Stelzer, P. Torrielli, and M. Zaro. The automated computation of tree-level and next-to-leading order differential cross sections, and their matching to parton shower simulations. 2014.

[5] I. Antcheva, M. Ballintijn, B. Bellenot, M. Biskup, R. Brun, N. Buncic, Ph. Canal, D. Casadei, O. Couet, V. Fine, L. Franco, G. Ganis, A. Gheata, D. Gonzalez Maline, M. Goto, J. Iwaszkiewicz, A. Kreshuk, D. Marcos Segura, R. Maunder, L. Moneta, A. Naumann, E. Offermann, V. Onuchin, S. Panacek, F. Rademakers, P. Russo, and M. Tadel. Root a c++ framework for petabyte data storage, statistical analysis and visualization. *Computer Physics Communications*, 180(12):2499 – 2512, 2009. 40 YEARS OF CPC: A celebratory issue focused on quality software for high performance, grid and novel computing architectures.

[6] The ATLAS Collaboration. The ATLAS experiment at the CERN large hadron collider. *Journal of Instrumentation*, 3(08):S08003–S08003, aug 2008.

[7] T. Gleisberg, S. Hoeche, F. Krauss, M. Schoenherr, S. Schumann, F. Siegert, and J. Winter. Event generation with sherpa 1.1. 2008.

[8] Paolo Nason and Carlo Oleari. Nlo higgs boson production via vector-boson fusion matched with shower in powheg. 2009.

[9] Carlo Oleari. The powheg-box. 2010.

[10] Torbjrn Sjstrand, Stefan Ask, Jesper R. Christiansen, Richard Corke, Nishita Desai, Philip Ilten, Stephen Mrenna, Stefan Prestel, Christine O. Rasmussen, and Peter Z. Skands. An introduction to pythia 8.2. 2014.

[11] M. zur Nedden. The LHC run 2 ATLAS trigger system: design, performance and plans. *Journal of Instrumentation*, 12(03):C03024–C03024, mar 2017.